ORIGINAL ARTICLE

Ultra-high performance concrete and fiber reinforced concrete: achieving strength and ductility without heat curing

**Kay Wille · Antoine E. Naaman ·
Sherif El-Tawil · Gustavo J. Parra-Montesinos**

Abstract Ultra-high performance concrete (UHPC) and ultra-high performance fiber reinforced concrete (UHP-FRC) were introduced in the mid 1990s. Special treatment, such as heat curing, pressure and/or extensive vibration, is often required in order to achieve compressive strengths in excess of 150 MPa (22 ksi). This study focuses on the development of UHP-FRCs without any special treatment and utilizing materials that are commercially available on the US market. Enhanced performance was accomplished by optimizing the packing density of the cementitious matrix, using very high strength steel fibers, tailoring the geometry of the fibers and optimizing the matrix-fiber interface properties. It is shown that addition of 1.5% deformed fibers by volume results in a direct tensile strength of 13 MPa, which is 60% higher than comparable UHP-FRC with smooth steel fibers, and a tensile strain at peak stress of 0.6%, which is about three times that for UHP-FRC with smooth fibers. Compressive strength up to 292 MPa (42 ksi), tensile strength up to 37 MPa (5.4 ksi) and strain at peak stress up to 1.1% were also attained 28 days after casting by using up to 8% volume fraction of high strength steel fibers and infiltrating them with the UHPC matrix.

K. Wille (✉)
Department of Civil and Environmental Engineering,
University of Connecticut, 261 Glenbrook Road,
Storrs, CT 06269-2037, USA
e-mail: kwille@engr.uconn.edu

A. E. Naaman
Department of Civil and Environmental Engineering,
University of Michigan, 2340 G.G. Brown Building,
Ann Arbor, MI 48109-2125, USA

S. El-Tawil
Department of Civil and Environmental Engineering,
University of Michigan, 2374 G.G. Brown Building,
Ann Arbor, MI 48109-2125, USA

G. J. Parra-Montesinos
Department of Civil and Environmental Engineering,
University of Michigan, 2370 G.G. Brown Building,
Ann Arbor, MI 48109-2125, USA

1 Introduction

Concrete or cementitious composites with compressive strength over 150 MPa (22 ksi) are generally described as ultra-high performance concrete (UHPC); if fibers are added in order to decrease brittleness and increase energy absorption capacity the term ultra-high performance fiber reinforced concrete (UHP-FRC) is used. UHPC's high compressive strength, obtained through dense particle packing, implies high durability, improved resistance against freeze-thaw cycles and

various chemicals as well as higher penetration resistance. UHPCs have also been reported [12] not to be susceptible to alkali-silica reaction (ASR). These special material properties make them particularly suitable for durable, resilient, and blast and impact resistant structures.

Since the appearance of effective dispersants for cement systems around the 1970s, many researchers have attempted to achieve record compressive strengths by decreasing the porosity of cementitious materials. Yudenfreund et al. [35] achieved a compressive strength of 230 MPa (33 ksi) on low porosity cement paste specimens using a vacuum mixing process. Hot temperature and pressure technique was first applied by Roy et al. [28], obtaining a compressive strength of 510 MPa (74 ksi) by using a pressure of 50 MPa (7.3 ksi) and temperatures of up to 250°C (480°F). Compressive strengths over 200 MPa (30 ksi) were also achieved with polymer modified cementitious materials, referred to as macro-defect-free (MDF) cements [6] or with slurry infiltrated fiber concrete (SIFCON) with fiber volume fractions of up to 10% [22].

Bache [3] introduced densified small particles (DSP), whose porosity was decreased by incorporating microsilica and superplasticizer in the mix design. This led to compressive strengths between 120 and 250 MPa (17–36 ksi). In 1995, Richard and Cheyrezy [25] introduced reactive powder concrete (RPC) and reported compressive strengths up to 800 MPa (116 ksi), using a temperature of up to 400°C (750°F), pressure of 50 MPa (7.3 ksi), 10% volume fraction of steel fibers, and steel aggregates.

Both high temperature heat curing and pressure are considered impractical treatments for bulk applications by the concrete profession. Thus, while some researchers have been very interested in developments and investigations on RPC [1, 4, 11, 18, 19, 29, 30], others have attempted to achieve compressive strengths greater than 150 MPa (22 ksi) without heat curing [5, 13, 16, 17, 20].

In a prior study, Wille et al. [34] have shown that, by following basic rules for mix design, the spread value in accordance to ASTM C 230/C 230M can be used as a quick indicator to optimize ultra-high performance cementitious paste, which consists of cement (C), water (W), silica fume (SF), glass powder (GP) and superplasticizer (SPL). It is understood that an increase in the spread value achievable by changing the type of

material within its class, and/or by changing the materials proportions indicates an improved particle packing while the amount of water is kept constant. Therefore the amount of water and thus the W/C ratio can be reduced while maintaining workability. This leads to an increase in compressive strength. Simply reducing the W/C ratio while not having a higher packing density leads to a decrease in workability and an increase in the amount of entrapped air, and thus, no enhancement in compressive strength. From the results of 38 UHP pastes, Wille et al. [34] showed that the compressive strength can be related to the product $(W/C) \times air^{1/3}$ where air represents the percentage of "entrapped air" (Fig. 1). They also made recommendations for the most appropriate materials for UHPC available on the US market which led to a UHPC mixture with compressive strength over 190 MPa (27.5 ksi) after 28 days without special heat curing or pressure (UHPC A in Table 1).

The main goal of this research was to design UHP-FRCs with more than 200 MPa in compressive strength, more than 10 MPa in post-cracking tensile strength and an associated post-cracking strain capacity of at least 0.3% (which exceeds the yield strain of commonly used steel reinforcement). Tensile strengths in excess of the first cracking strength of the matrix are necessary to achieve multiple cracking, which is the key factor for a higher tensile strain at peak stress and thus, more ductility.

The proportions of the designed UHP-FRC mixtures are given in Table 1. The selection of related materials and the strategy pursued are described
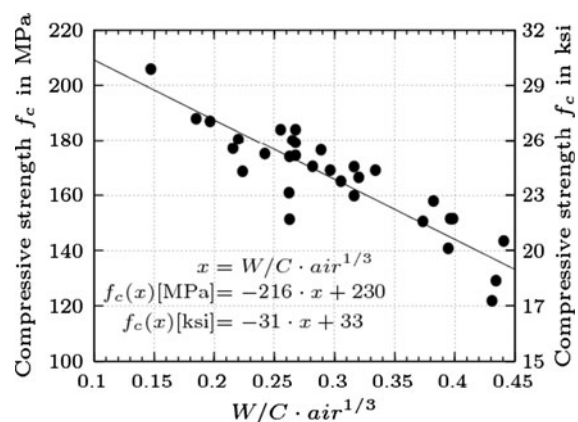

Fig. 1 Effect of W/C ratio in combination with air content on compressive strength

Table 1 Recommended mixtures for UHPC and UHP-FRC

Type	UHPC				UHP-FRC				
	A[a]	B[a]	C	D	A[a]	B[a]	C	D	SifCon
Cement	1.00	1.00	1.00	1.00	1.00	1.00	1.00	1.00	1.00
Silica fume	0.25	0.25	0.25	0.25	0.25	0.25	0.25	0.25	0.25
Glass powder	0.25	0.25	0.25	0.25	0.25	0.25	0.25	0.25	0.25
Water	0.220	0.195	0.190	0.180	0.212	0.200	0.185–0.195	0.18–0.20	0.207
Superplasticizer[b]	0.0054	0.0108	0.0108	0.0114	0.0054	0.0108	0.0108	0.0108	0.0108
Sand A[c]	0.28	0.30	0.31	1.05	0.27	0.28	0.29	0.92	0.76
Sand B[d]	1.10	0.71	0.72	0.00	1.05	0.64	0.67	0.00	0.00
Ratio Sand A/B	20/80	30/70	30/70	100/0	20/80	30/70	30/70	100/0	100/0
Fiber	0.00	0.00	0.00	0.00	0.15/0.25	0.22	0.18–0.27	0.22–0.31	0.71
Fiber in vol.%	0	0	0	0	1.5/2.5	2.5	2.0–3.0	2.5–3.5	5[e]/8[f]
$f'_c[cube, 28d]$ MPa	194	207	220–240	232–246	207/213	219	227–261	251–291	270[e]/292[f]
$f_t[tension]$ MPa	6.1 –7.4[g]	6.9 –7.8[g]	7.4 –8.5[g]	8.2–9.0[g]	8.2/14.2	15	16–20	20–30	37[e]

[a] Non vibrated, non surface cut

[b] Solid content

[c] Max. grain size 0.2 mm (1/128 in.)

[d] Max. grain size 0.8 mm (1/32 in.)

[e] Twisted (T) fiber

[f] Straight (S) fiber

[g] At first cracking, followed by immediate failure

below. To achieve the observed properties, the cementitious matrix was first optimized in terms of its compressive strength; very high strength steel fibers were used; and the fiber-matrix interfacial properties (bond) were tailored, through changes in fiber geometry, to improve mechanical bond.

2 Definition

To the writers' knowledge the term "ultra-high-performance concrete" was first used in a publication by de Larrard and Sedran [7]. In spite of two recent symposia on the subject, there is no general agreement as to the definition of UHPC [9, 10]. Using information from Rossi [26, 27] and two symposia proceedings [9, 10], the following definition, which was adopted at the onset of this investigation, is suggested:

> Ultra-high performance concretes (UHPCs) use a relatively high binder ratio, a water to cementitious ratio (or water to binder ratio) less than 0.2, and show a compressive strength in excess of 150 MPa (22 ksi).

It is understood that the resulting composite has a very high packing density, leading to significantly higher durability compared to conventional concrete. For consistency and comparison purposes, the compressive strength should be based on a standardized specimen and test procedure (see [11]).

3 Research significance

In order to build longer span bridges, taller buildings and more sustainable and durable reinforced concrete structures, it is becoming imperative to design cementitious materials with improved compressive and tensile strength, enhanced durability and superior ductility while maintaining small crack width under tensile loading. The UHPC and UHP-FRC mixtures developed in this study which required neither heat curing, nor pressure curing, nor a special mixer, help respond to that need and facilitate on-site applications by providing composites that are significantly more cost effective than the currently available alternatives on the market.

4 Experimental program

An intensive research program was conducted to achieve the objectives of the study. The following tests were carried out:

(1) *Spread value and compression tests*: A minimum in matrix porosity and thus, a maximum in compressive strength were sought by evaluating spread values in the fresh state and compressive strengths in the hardened state of different matrix compositions and proportions. Based on the results of 38 different UHP pastes [34] the most appropriate materials (cement, silica fume, glass powder, superplasticizer) for UHPC available on the US market were selected. To increase the matrix particle packing, the amount of SF, the amount and the median particle size of GP as well as the ratio between fine Sand A and fine Sand B were investigated (Table 2).

(2) *Single fiber pull out tests*: Single fiber pull out tests provide valuable information in order to optimize the UHP-FRC tensile behavior. Because of space limitation, the pull-out test program cannot be described in details; here, only the most important conclusions are pointed out regarding interfacial properties between matrix and fiber as well as the mechanical bond which was optimized by tailoring the fibers' shape and geometry.

(3) *Direct tensile tests*: Over 250 direct tensile tests were performed to evaluate and optimize the tensile behavior of UHP-FRC composites in terms of strength, ductility and energy absorption. In comparison to single fiber pull out tests, the tensile tests additionally incorporate the fiber group effect, fiber volume fraction as well as fiber orientation and distribution. Only some selected results are provided here.

(4) *Bending tests*: To compare the bending behavior with the direct tensile behavior, selected UHP-FRCs have been tested in bending according to ASTM 1609 [2].

4.1 Mixture design strategy and mixing procedure

Investigating the spread value through a flow cone test can help fine-tune the mixture in its proportions,

particle size distribution, and selection of best components from an available set. To increase the flowability of the paste while maintaining the amount of water constant (or to maintain the same flowability while reducing water content), the packing density has to be increased such that the volume of water-filled voids is reduced. Therefore, less water would be physically trapped, making more of the remaining water available to cover the surface of the particles. This would increase the thickness of the water film on the surface of the particles and decrease the overall viscosity of the paste. Thus, by improving the rheological behavior, the W/C ratio can be reduced to maintain the same workability (spread value), which is one of the key conditions to achieve a UHPC.

In order to improve packing density (thus compressive strength), evaluated indirectly through a flow cone test, the following basic rules were followed.

- Usage of C for hydration
- Usage of pozzolanic reactive material, preferable SF, with a particle size of about 5–20 times less than that of cement
- Usage of very fine GP as filler, with particle size between that of C and SF. Herein, GP is considered a non-reactive material, although there is some evidence that very fine glass powder reacts with the cement paste under heat treatment [21].
- Usage of fine sand with a grain size distribution selected for maximum bulk density
- Minimization of particle agglomeration through the mixing procedure and the incorporation of SPL

An optimization of different components and their proportions was typically followed to generate a UHPC. The required effort was reduced by focusing first only on the flow characteristics of the paste. In a second step, two types of fine unground sands, named Sand A and Sand B, were added in various proportions to achieve an optimized UHPC. Sand A had a maximum grain size of 0.2 mm (1/128 in.) and a mean size of 0.11 mm (0.004 in.), and Sand B had a maximum grain size of 0.8 mm (1/32 in.) and a mean grain size of 0.5 mm (0.02 in.). In a third step, high strength ($\sigma_{fu} \geq 2100$ MPa [304 ksi]) steel fibers with various geometry (Table 3) and volume fraction were added to the mix to achieve optimized UHP-FRCs.

Table 2 Experimental program

Parameter	Range	Material	Test
Preselecting of materials and pre proportioning [34]			
Different types of C, SF, SPL, various W/C ratios and paste proportions	38 mixtures	Paste	SV, CT
Fine sand ratio (Sand A/Sand A + B)	0–1.0	Sand	
Fine-tuning of mix proportion for UHPC			
Amount of SF (C:SF)	1:0–1:0.3	Paste	SV, CT
Amount of GP (C:SF:GP)	1:0.25:0–1:0.25:0.5	Paste	SV, CT
Fine sand ratio (Sand A/Sand A + B)	0–1.0	UHPC	SV, CT, SFPOT
Particle size of GP (d_{50} in μm)	1.7, 3.4, 5.0	UHPC	SV, CT, SFPOT
Type of SPL, SF	–	UHPC	SV, CT, SFPOT
Optimizing tensile behavior of UHP-FRC			
Fiber shape	Smooth (S), hooked (H), twisted (T)	UHPC	SV, SFPOT, TT
Fiber diameter (mm)	0.12–0.3	UHPC	SV, SFPOT, TT
Fiber length (mm)	6–30	UHPC	TT
Fiber volume fraction (%)	0–5 (SifCon)	UHPC	SV, TT
Analysing bending behavior of UHP-FRC			
Fiber shape	Smooth (S), hooked (H), twisted (T)	UHPC	3PBT

SV spread value, *CT* compressive test, *SFPOT* single fiber pull out test, *TT* tensile test, *3PBT* 3-point bending test

Table 3 Properties of high strength steel fibers used in this study

Notation	Form	Number of twists	d_f, mm	l_f, mm	l_f/d_f	Tensile strength, MPa (ksi)
S	Straight (S)	0	0.20	13	65	≈2600 (377)
H	Hooked (H)	0	0.38	30	79	≈2900 (420)
T_1	High twisted (T_1)	16	0.30[a]	30	100	≈2100 (304)
T_2	Low twisted (T_2)	6–8	0.30[a]	30	100	≈3100 (449)

[a] Manufactured out of round wire with $d_f = 0.30$ mm, shaped into prism a/b = 0.24/0.30 mm

The optimization of fiber-matrix interface properties and mechanical bond was supported by single fiber pull-out tests.

The mixing procedure adopted in this research followed these steps: (1) SF and all the sand are dry mixed for about 5 min, (2) C and GP are added and mixed for at least another 5 min, (3) then water and SPL are added separately. The UHPC mixture becomes fluid approximately 5 min after the addition of water and SPL. Fibers, if any, were then added during the following 5 min. A horizontal pan mixer (capacity of around 60 l, 1.8 kW) with constant mixing (60 rpm), was found adequate for mixing the UHP-FRCs developed in this research. For smaller batches a food-type mixer (capacity of 5.6 l, rotational speed I/II equal to 136/281 rpm for agitator and 60/124 rpm for paddle) was used.

4.2 Mix preparation and testing

The paste was defined as the mixture containing all ingredients having particle size less than 50 μm. Therefore, the paste contained only C, SF and GP, which were thoroughly mixed prior to the addition of water and SPL. After mixing the paste, UHPC (with the addition of fine sand) or UHP-FRC (with the addition of fibers) were poured in a cone to full capacity in accordance to ASTM C 230/C 230M. The cone was then removed, allowing the paste to spread on the plate while the plate remained steady. After ½ min, the spread was measured. At the same time as the flow test was conducted, a number of 50 mm (2 in.) cubes for compressive tests, 5 half dogbone shaped specimens for single fiber pull out tests, 3–6 dogbone shaped specimens for tensile tests and three

small bending beams for 3 point bending tests were prepared. These specimens were demolded after 24 h and water cured at 20°C (68°F) until 1 day before testing.

Specimen preparation for testing compressive strength in this part of the study differed from the previous one [34] in the following way:

- Paste was mixed at variable mixing speed, which improved particle distribution.
- Moderate vibration was applied during casting, which led to reduced air entrapment.
- Cube molds (2 in.) were used for casting specimens, which were easier to prepare.
- The top layers of the specimens (about 2 mm) were cut off to ensure that the weak zone did not influence the results.

Although the cubes had a relative even and smooth surface, their loading faces were ground prior to testing to ensure test results with high consistency. No capping of specimens was performed because of the limited strength (100 MPa or 14.5 ksi) of the available capping material.

5 Experimental results on paste and UHPC

5.1 Proportioning of paste

As mentioned earlier, optimization of mixture constituents and proportions was performed based on results from flow cone tests as described in [34]. The reduction of the W/C ratio during the mix development phase from 0.30 to 0.17, while maintaining a spread value of approximately 270 mm (10.6 in.), led to an increase in compressive strength from 122 MPa (17.7 ksi) to 177 MPa (25.7 ksi). A maximum paste compressive strength of 206 MPa (29.9 ksi) was attained at minimum of $(W/C) \times air^{1/3}$ (Fig. 1). These results confirmed the suitability of the simple flow cone test as an indirect indicator of packing density, and thus compressive strength. The addition of fine Sand A and fine Sand B in the proportion 20/80 led to UHPC A (Table 1) with a compressive strength of 194 MPa (28.1 ksi) characterized by self-consolidating properties.

In order to fine tune the paste proportions, the amounts of SF and GP were investigated separately.

To find the optimum amount of SF evaluated by spread value and cube compressive strength the proportion of C:SF was investigated in the range of 1:0 to 1:0.3 while keeping the water to powder ratio (W/P) constant (W:[C + SF] = 0.166). For each mixture, two spread tests and three cube compressive strength tests were performed and their average values calculated.

The results in Fig. 2a and Table 4 indicate that by increasing the amount of SF, the spread value increases from 275 mm (0% SF) to a maximum of 365 mm (25% SF). Note that despite the smaller particle size of SF vs. C the increase in spread is significant. This confirms the increase in packing density through the addition of SF up to 25% of C by weight. The associated compressive strength results follow the same trend, that is from a minimum of 158 MPa for the mixture without SF to a maximum of 229 MPa with C:SF = 1:0.25. The reason for the increase in compressive strength of about 45% can be explained by the pozzolanic reaction of SF, the lower air content due to the better flowability, and improved packing density. The optimum amount of SF with regard to the fresh and hardened paste properties was found to be 25% of C by weight.

Based on the optimal proportion of C:SF = 1:0.25 the amount of GP was then varied in the range of C:SF:GP = 1:0.25:0 to C:SF:GP = 1:0.25:0.5. Because of the previously obtained very flowable mixtures, the W/P ratio was lowered and kept constant at W/P = 0.144 (Table 4). In comparison to the prior investigation, where the weight replacement of C by SF led to a significant increase in spread and strength, the replacement of C + SF by GP results in a minor increase in strength, while the workability is kept constant (Fig. 2b). A significant loss of flowability was observed with a proportion of C:SF:GP = 1:0.25:0.5, so that W/P had to be increased to W/P = 0.166 to get a comparable spread value for the compressive strengths tested. The associated compressive strength was increased from 221 MPa (0% of GP) to 240 MPa (C:SF:GP = 1:0.25:0.3), that is, an increase of 9%. The optimum amount of GP can be considered in the range of 20–30% of C.

The previously observed optimal powder proportion of C:SF:GP = 1:0.25:0.25 found in [34] was confirmed with this part of the study and was used for all UHPCs and UHP-FRCs described here.
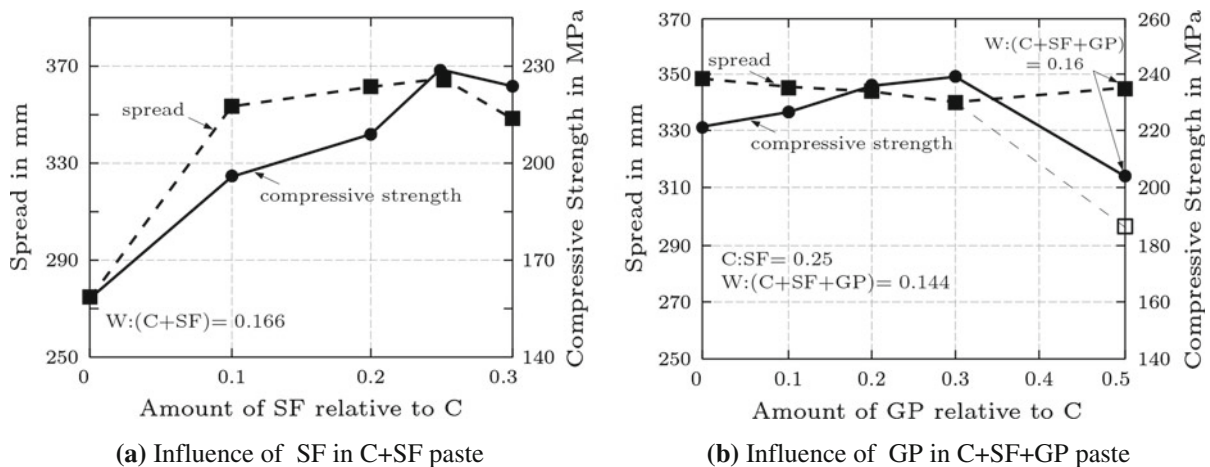
(a) Influence of SF in C+SF paste

(b) Influence of GP in C+SF+GP paste

Fig. 2 Influence of the amount of: **a** SF and **b** GP in the paste on fresh and hardened properties

5.2 Mix design of UHPC

Adding only fine sand to the paste led to the final mixture. Investigation of the bulk density of various mixtures of Sand A ($d_{50} = 0.11$ mm) and Sand B ($d_{50} = 0.5$ mm) was conducted to optimize their proportion. An optimum content of Sand A ranging between 30 and 50% was observed (Fig. 3a). Whereas partially replacing Sand B by Sand A resulted in a higher bulk density, it also increased the demand for water due to the larger surface area of the smaller particles of Sand A. Thus further investigation of UHPC mixtures was performed using spread and compressive strength results in order to obtain the optimum proportion of Sand A to Sand B. For this, UHPC B (Table 1) was used with a variation in the

sand proportion Sand A/Sand (A + B) from 0 to 1. Figure 3b indicates that the spread values follow the same trend as previously obtained from the bulk density, that is, with the addition of Sand A the spread and the bulk density increase up to a maximum (around 30%/70% of Sand A to Sand B). A further increase of Sand A to 50% and 100% of Sand A + B results in a decrease in the spread value and bulk density. The compressive strength results follow the same trend up to maximum spread value, that is, with increasing the amount of Sand A, the compressive strength increases. Despite the loss in workability due to a further replacement of Sand B by Sand A, the compressive strength slightly increased. The reason for this behavior is attributed to the fact that the smaller maximum particle size (0.25 mm

Table 4 Mixtures and test results for pastes in order to optimize proportion

C:SF:GP	SPL, % of C	Solid SPL, weight	W/C	W/P	Spread, mm	$f'_c[prism]$[a], MPa (ksi)
Amount of SF						
1:0:0	2.31	0.93	0.166	0.166	275	158 (22.9)
1:0.1:0	1.76	0.70	0.178	0.166	353	196 (28.4)
1:0.2:0	1.35	0.54	0.192	0.166	362	209 (30.3)
1:0.25:0	1.35	0.54	0.200	0.166	365	229 (33.1)
1:0.3:0	1.35	0.54	0.208	0.166	349	224 (32.4)
Amount of GP						
1:0.25:0	1.35	0.54	0.180	0.144	349	221 (32.0)
1:0.25:0.1	1.35	0.54	0.195	0.144	345	227 (32.9)
1:0.25:0.2	1.35	0.54	0.209	0.144	344	236 (34.2)
1:0.25:0.3	1.35	0.54	0.223	0.144	340	240 (34.7)
1:0.25:0.5	2.02	0.81	0.280	0.160	345	204 (29.5)

[a] Average compressive strength at 28 days, 1 in. = 25.4 mm
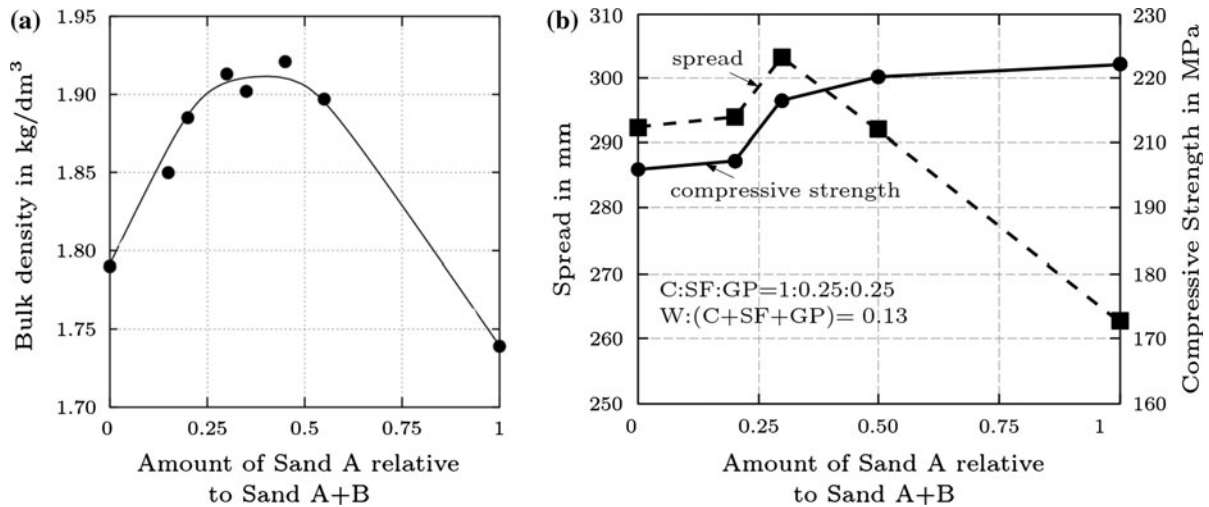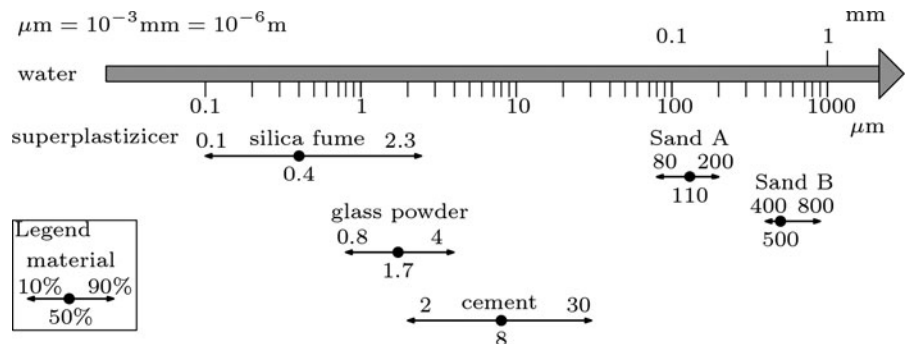
Fig. 3 Influence of ratio Sand A/Sand A + B on bulk density, spread value and compressive strength of UHPC. **a** Bulk density of mixed sands and **b** spread value and compressive strength

instead of 0.8 mm) causes less stress concentration and might have fewer flaws in the crystalline structure than larger particles. It can be generally concluded that investigating the bulk density of sand mixtures is an easy and quick method for optimizing the packing of particles having a maximum size larger than the paste constituents.

Figure 4 shows a logarithmic scale with the grain size distribution of the materials used in the mixtures recommended in Table 1. The data shown in this figure provide a good idea of the particle packing. Additional information about recommended properties and proportions for the various materials used is summarized in Fig. 5. It can be observed that the optimization of paste proportions allowed a substantial reduction in the amount of superplasticizer needed for adequate workability (about 1% of cement weight).

Very low W/C ratio and high amount of cement raises the concern of high autogenous shrinkage. The study of autogenous shrinkage of UHPCs and UHP-FRCs was beyond the scope of this research. Results from research by Dudziak and Mechtcherine [8], however, indicate that autogenous shrinkage strains in non-heated UHPCs (in the order of 700×10^{-6}) could be decreased by 75% (to approximately 175×10^{-6}) through the use of super absorbent polymers that provide water for internal curing without significantly changing the mix design.

5.3 Role of particle size of GP and SF and particle dispersion quality

The appearance of effective dispersants for cement particles in the 1970s has played a key role in the development of low porosity cementitious materials
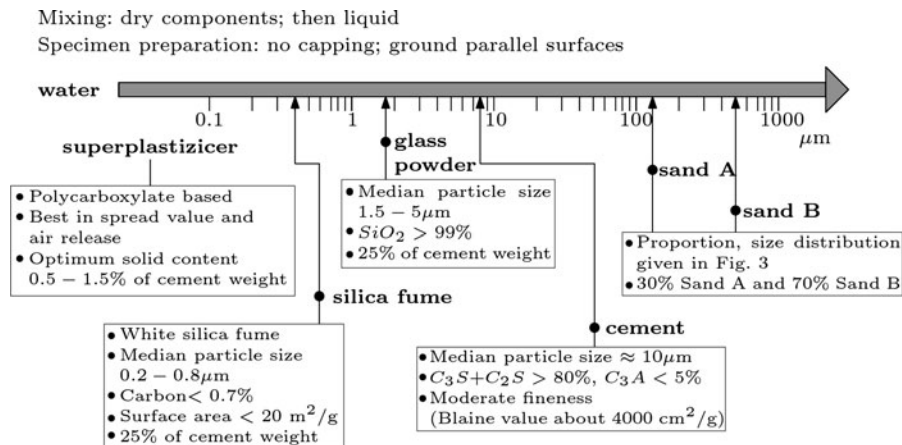
Fig. 4 Median and range of particle size distribution (10, 90%) for all particles used in the mix design (in mm)

Mixing: dry components; then liquid
Specimen preparation: no capping; ground parallel surfaces

Fig. 5 Recommended mix design parameters

accompanied with a low W/C ratio and associated with a high compressive strength. The SPL used for UHPC A was selected out of seven different SPL by investigating air release and flowability of paste mixtures. While most SPL are designed for a better dispersion of cement particles, a SPL was sought that is able to interact with all fine particles (C, SF, GP) and thus improves their dispersion ability. With further investigation of fine particle-SPL interaction, a SPL could be selected, which ideally worked together with the paste constituents. While the workability of UHPC was kept constant, the W/C ratio could be further reduced from 0.22 (UHPC A) to 0.19 (UHPC C) by replacing the SPL and thus, by providing a better dispersion quality of all particles. This led to an increase in material compressive strength by about 10–15%.

In order to further increase particle packing a very fine filler (herein GP) with median particle size between that of C (herein $d_{50} = 8$ μm) and SF (herein $d_{50} = 0.4$ μm) was used. Different median particles sizes ($d_{50} = 1.7, 3.4, 5.0$ μm) of GP were investigated for their influence on spread value and compressive strength of an UHPC similar to UHPC C. Three conclusions can be drawn from the observed results (Fig. 6): (1) Compressive strength does not change significantly when the median particle size of GP varies from about 1.7–5 μm, but it tends to be slightly higher with smaller particle size, (2) The change in spread follows the same trend as the change in strength confirming again the usefulness of the spread test in order to optimize particle packing, (3) Generally fine materials with a
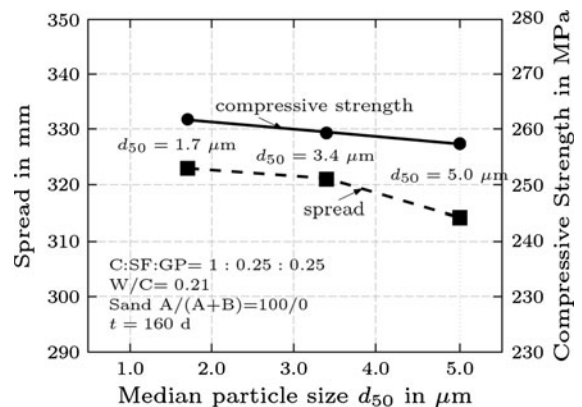

Fig. 6 Influence of median particle size of GP on spread value and compressive strength

larger median particle size demand less water and this leads to a better workability, if the amount of water is kept constant in the mix. However, the UHPC with the "coarsest" GP (5 μm) resulted in a spread loss in comparison to UHPC with GP of 1.7 μm. The increased interference of the large GP particles (5 μm) with the cement particles (8 μm) may be the reason for a decrease in spread value indicating a decrease in packing density. Further enhancement in particle packing density was achieved by replacing the selected SF ($d_{50} = 0.4$ μm [updated]) [34] by another white silica fume with a median particle size of ($d_{50} = 0.5$ μm) and with a low carbon content, but currently not commercially available in the US. Incorporating that SF in the mix led to an improved workability so that the W/C ratio could be reduced to 0.18 without adversely affecting the workability of

the mix. It resulted in a compressive strength of 246 MPa (35.7 ksi) under laboratory conditions, without special heat or pressure curing treatment.

5.4 Comparison of non heated and moderately heated UHPCs

Figure 7 compares the compressive strength of the UHPCs and UHP-FRCs developed in this study, with over 60 different UHPCs and UHP-FRCs tested worldwide. The results in Fig. 7 were taken from the proceeding of two international symposia on UPHC [9, 10]. Sorting the test results into different groups illustrates, that the compressive strength of UHPC can be increased: (1) by incorporating basalt aggregate in the mix design, (2) by adding fibers to the mix, (3) by significantly reducing the amount of entrapped air (vacuum mixing) and (4) by treating the specimens with moderate heat (90°C/194 F). Results on heat treated specimens in excess of 90°C were not included.

The compressive strength results of the UHPCs (up to 246 MPa) and UHP-FRCs (up to 291 MPa) designed in this study show very high strengths in their group and are comparable to the strength results obtained by others with moderate heat treatment. It can be concluded from Fig. 7 that the goal sought in this study to develop competitive UHPC and UHP-FRC mixtures without using heat or pressure curing or a special mixer in order to facilitate increased applications has been attained through mix design optimization.

6 Experimental results on fiber matrix interaction

6.1 Influence of matrix design on pull out behavior of smooth steel fibers

Single fiber pull out tests were performed to calculate the fiber matrix bond properties and to efficiently optimize the tensile behavior of UHP-FRC. Detailed information on the test set up (Fig. 8a) and the pull out behavior of smooth fibers with $l_f/d_f = 13/0.2$ mm and an embedded length, $L_E = 6.5$ mm, can be found in [31]. Figure 8b compares the shear stress vs. relative slip relationship of smooth fibers embedded in high strength concrete (HSC) with compressive strength of 60 MPa (8.7 ksi) [23] with the curves of different UHPCs of compressive strength up to 246 MPa (35.7 ksi). It can be observed that changing the surrounding matrix from HSC to UHPC results in a significant increase in shear stress resistance, accompanied by a hardening of the bond stress vs. slip curve.

The following effects may explain the bond-slip hardening behavior of smooth fibers: (1) wedge effect of adhered and abraded particles, (2) scratching of the fiber surface, such as delamination of the brass coating, and (3) fiber end deformation due to the

Fig. 7 Overview of UHPC compressive strength, summarized from different authors (Data taken from [9, 10])
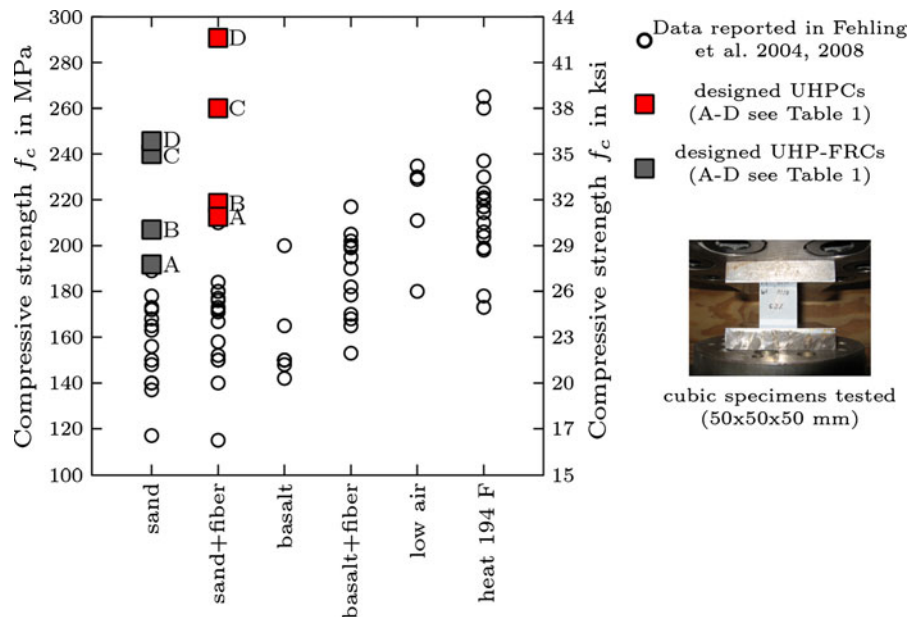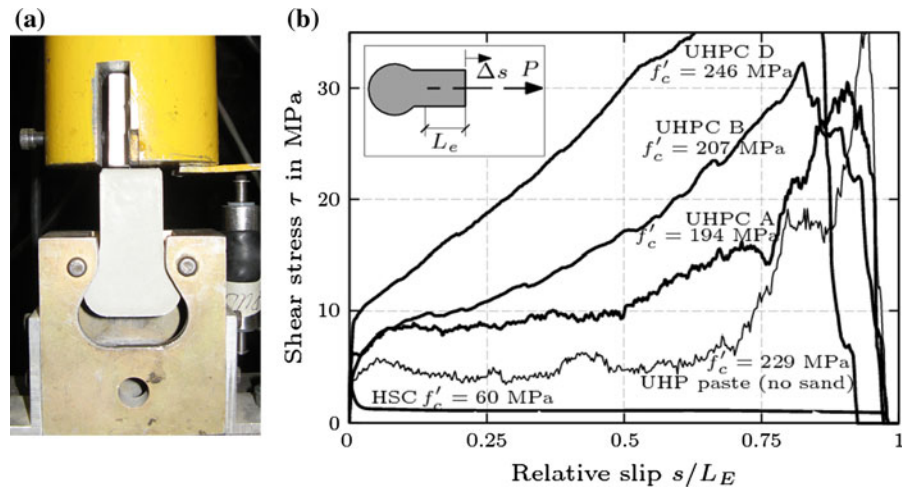
Fig. 8 Single fiber pull-out: **a** test set up and **b** Shear stress slip relationship of smooth (S) Fibers embedded in different cementitious matrices: HSC (60 MPa) and UHPC (up to 246 MPa)

cutting process. Improvement in particle packing through enhanced fine particle dispersion (UHPC B) and through decrease of smallest particle size (UHPC D) led to an improved bond slip hardening behavior and to equivalent bond strength up to 20 MPa, which is a key factor for high tensile strength and high ductility of UHP-FRC [31].

Pull out tests on single smooth steel fibers embedded in UHPC with different GP median particle sizes also showed that compressive strength is an important parameter, but not a sufficient condition for achieving best equivalent bond strength (Fig. 9). As shown in Fig. 6, the compressive strength of UHPC with different median particle sizes of GP does not change significantly. However, the shear stress resistance of the fiber pulled out of the UHPC

with the smallest GP median particle size is significantly increased, showing a more pronounced bond-slip hardening behavior. Based on these tests, all UHP-FRCs in this research were designed with GP of ($d_{50} = 1.7$ μm).

6.2 Influence of fiber geometry on pull out behavior

The fiber matrix bond mechanisms can be grouped into (1) physico-chemical bond based on adhesive and frictional forces, and (2) mechanical bond due to fiber deformation. In comparison to smooth fibers deformed fibers, such as end hooked or twisted fibers (Fig. 10) mechanically contribute an additional bond component, which increases the pull out resistance (Fig. 11).
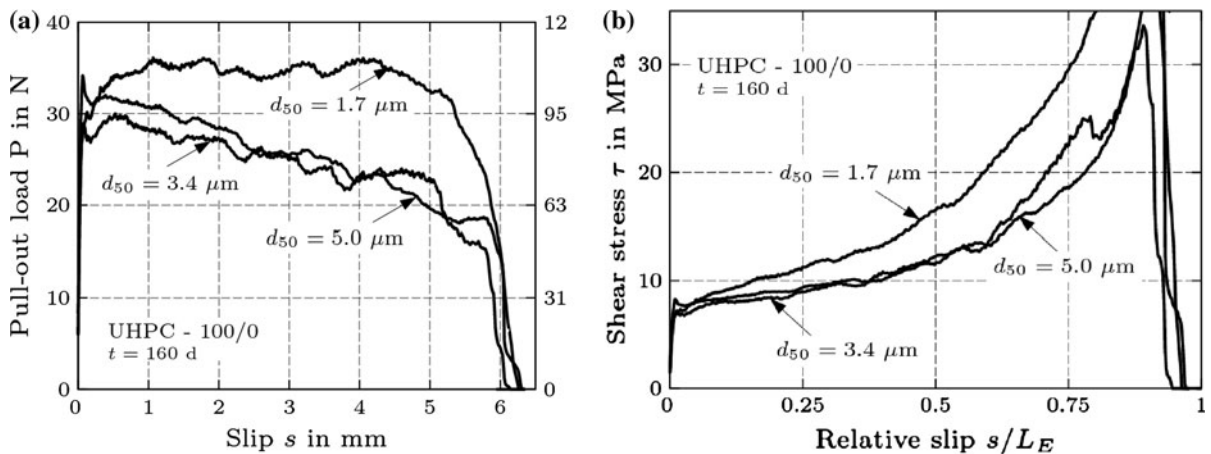

Fig. 9 Influence of GPs median particle size on interfacial properties. **a** Pull-out load slip relationship and **b** shear stress slip relationship

Fig. 10 Different types of steel fibers used in this research. **a** Straight smooth (S), **b** hooked (H) **c** high twisted (T1) and **d** low twisted (T2)
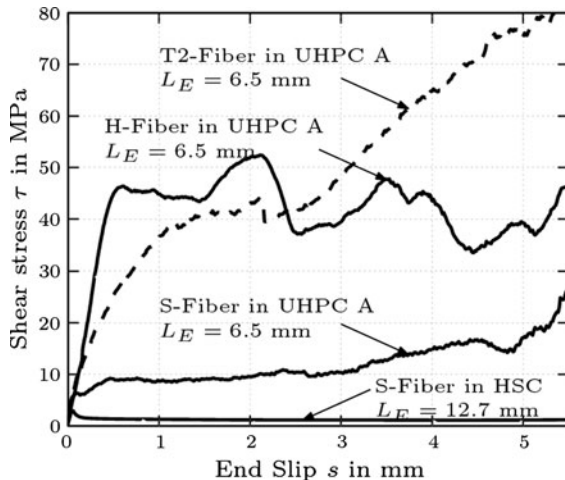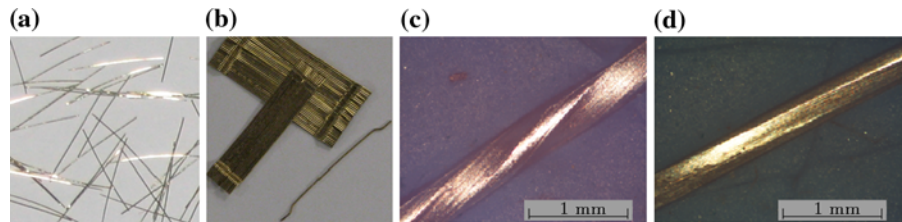

Fig. 11 Shear stress slip relationship of smooth (S) and deformed (T2, H) steel fibers embedded in HSC (60 MPa) and UHPC A (194 MPa)

Further, by tailoring the twist ratio of the twisted fiber, the bond vs. slip was improved in terms of equivalent bond strength and bond slip hardening [33].

7 Experimental results for UHP-FRC

UHP-FRCs can achieve ductile tensile behavior, if they are designed to withstand a tensile stress higher than the cracking strength of the matrix. This leads to tensile strain hardening behavior accompanied by multiple cracking up to peak stress as illustrated in Fig. 12.

Test results show that the following three parameters clearly influence tensile strength and ductility in presence of high strength steel fibers:

(1)   *matrix compressive strength*: Figure 13b shows that by increasing the matrix compressive strength, the tensile strength as well as the tensile strain at peak stress is increased.

(2)   *fiber geometry*: Tailoring the fiber geometry by properly shaping and twisting the fiber increases the tensile strength as well as the tensile strain at peak stress (Fig. 14)

(3)   *fiber volume fraction*: Increasing the fiber volume fraction of smooth and twisted fibers within a certain range increases the tensile strength as well as the tensile strain at peak stress (Fig. 15). In order to preserve a suitable workability of UHP-FRC without fiber clumping, it is recommended not to exceed a fiber factor of $\chi_f = \ell_f / d_f \times V_f = 2$ [24].

In some tests, simultaneously using a cementitious matrix with a compressive strength in excess of 240 MPa (34.8 ksi), high quality high strength twisted steel fibers, and a fiber volume fraction of 5% (which requires infiltration of the matrix, that is, SifCon process), led to a tensile strength of 37 MPa (5.4 ksi) accompanied by a tensile strain at peak stress of 1.1% (Fig. 16).

8 Typical bending behavior of UHP-FRC

Bending tests on UHP-FRC were performed as per ASTM 1609 [2] in order to confirm the effectiveness of the fiber geometry observed in the direct tensile tests. Load deflection curves are shown in Fig. 17b and compare very well with the tensile stress–strain curves shown in Fig. 14 for the same mixtures. Note that the ratio of equivalent bending strength to direct tensile strength ranges between 2.4 and 2.65.

9 Summary and conclusions

Building up on a prior research on an UHPC this research described the development of some UHP-FRC composites with high tensile strength and high ductility. In the first step the cementitious matrix was optimized in its packing density evaluated by the
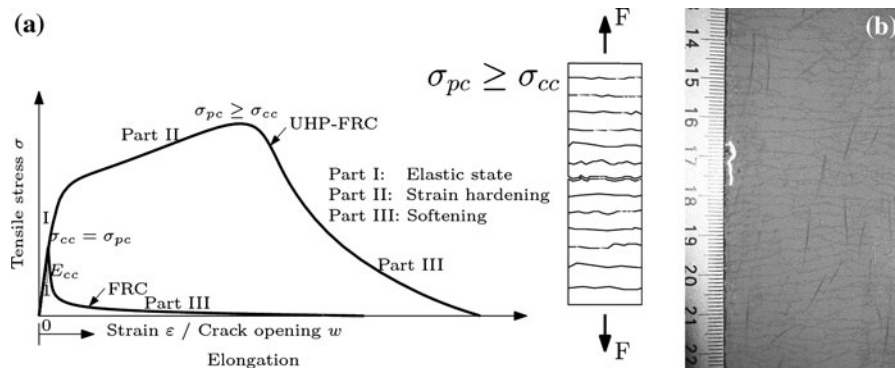
Fig. 12 **a** Strain hardening tensile behaviour and **b** multiple cracking UHP-FRC A (1.5% T)
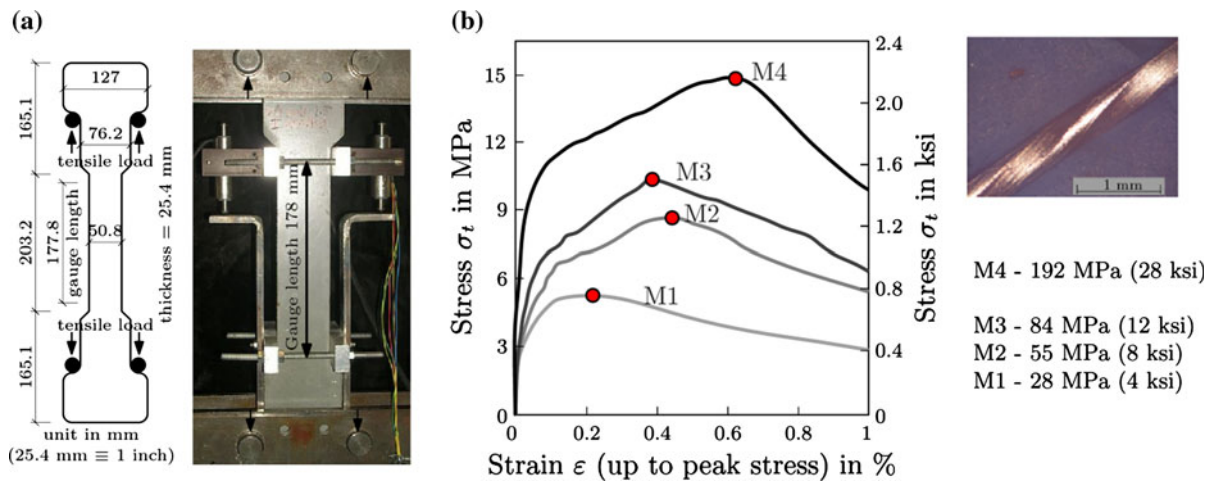

Fig. 13 Testing fiber reinforced concrete under uniaxial tensile loading. **a** Tensile test setup and **b** matrix strength dependent tensile behavior using high strength twisted steel fibers (from Kim et al. [14, 15])
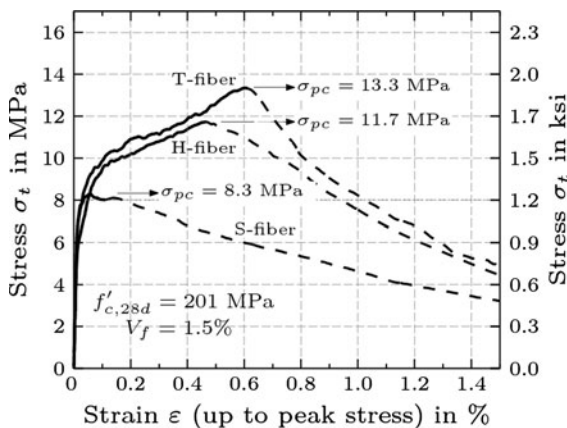

Fig. 14 Influence of fiber geometry on tensile behavior [32]

spread value and the compressive strength. The previously observed optimal powder proportion of cement:silica fume:glass powder of 1:0.25:0.25 found in [34] was confirmed and used for all UHPCs and UHP-FRCs described here. The UHPC mixtures developed have the additional benefit of being self-consolidating mixtures.

Parallel to the compressive tests, single fiber pull out tests were performed to investigate the fiber to matrix bond, to further optimize the matrix composition, to tailor the fiber geometry and to effectively design UHP-FRCs. The addition of 1.5% of high strength twisted steel fibers by volume led to a post-cracking tensile strength of 13 MPa (1.9 ksi), which is 60% higher than that of UHPC with smooth fibers,
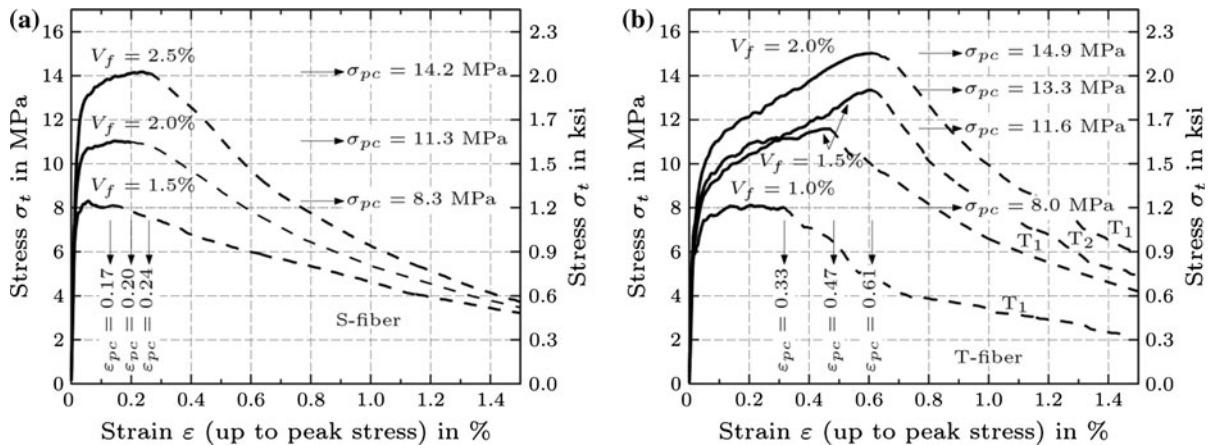
Fig. 15 Influence of fiber volume fraction on tensile behavior. **a** Smooth (S) fibers and **b** twisted (T) fibers [32]

Fig. 16 Tensile behavior of UHP-FRC using the SIFCON process (SifCon T)
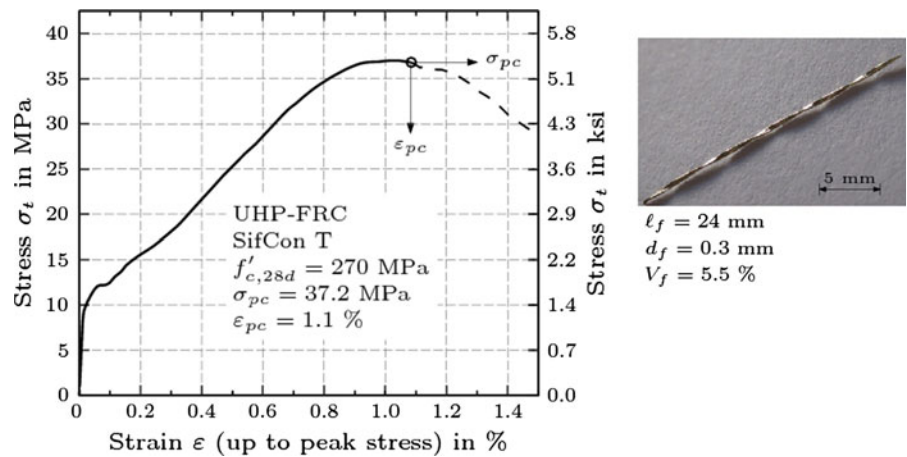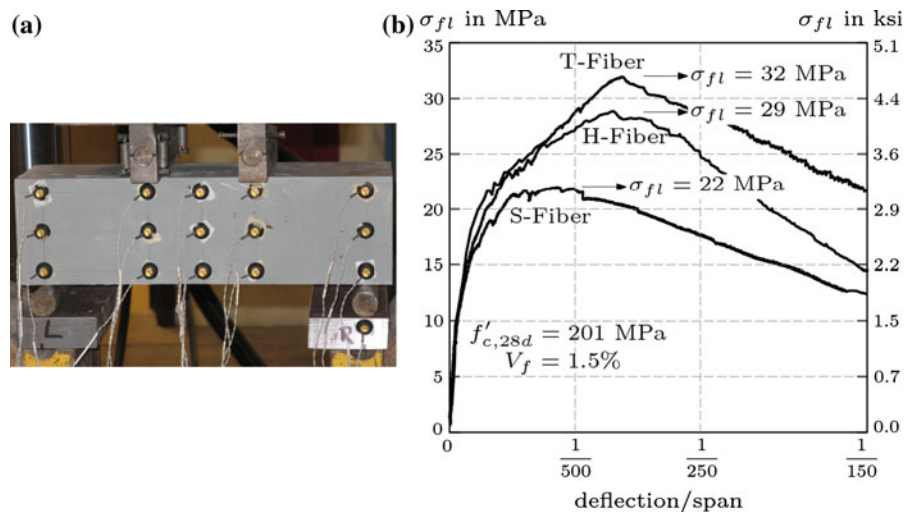

Fig. 17 UHP-FRC bending beam tests according to ASTM 1609 [2]. **a** Test set up and **b** influence of fiber geometry

and also to a tensile strain at peak stress of 0.6%, which is about three times that of UHPC with smooth fibers. Compressive strength up to 292 MPa (42 ksi), tensile strength up to 37 MPa (5.4 ksi) and strain at peak stress up to 1.1% were attained 28 days after casting, by using a volume fraction of high strength steel fibers up to 8% and infiltrating them with an ultra-high strength cementitious matrix. No special treatment such as heat curing, or pressure or special mixer was used.

It is hoped that this work will make UHPC and UHP-FRC more readily achievable to the research and professional community, and dispel the illusion that UHPC requires such special treatment or conditions that only the experts can succeed in it.

References

1. Ahlborn TM, Misson DL, Peuse EJ, Gilbertson CG (2008) Durability and strength characterization of ultra-high performance concrete under variable curing regimes. In: Second international symposium on ultra high performance concrete, Kassel, pp 197–204
2. ASTM C 1609/C 1609M – 05 (2005) Standard test method for flexural performance of fiber-reinforced concrete (using beam with third-point loading), ASTM International, West Conshohocken, PA, 8 pp
3. Bache HH (1981) Densified cement/ultrafine particle-based materials. In: 2nd int. conference on superplasticizers in concrete, Ottawa, 10–12 June 1981
4. Behloul M, Bernier G, Cheyrezy M (1996) Tensile behavior of reactive powder concrete (RPC). In: 4th international symposium on utilization of HSC/HPC, BHP'96, vol 3. Presses de l'ENPC, Paris, pp 1375–1381
5. Benson SDP, Karihaloo BL (2005) CARDIFRC—development and mechanical properties. Part III: uniaxial tensile response and other mechanical properties. Mag Concr Res 57:433–443
6. Birchall JD, Howard AJ, Kendall K (1981) Flexural strength and porosity of cements. Nature 289:388–390
7. de Larrard F, Sedran T (1994) Optimization of ultra-high-performance concrete by the use of a packing model. Cem Concr Res 24:997–1009
8. Dudziak L, Mechtcherine V (2008) Mitigation of volume changes of ultra-high performance concrete (UHPC) by using super absorbent polymers. In: Fehling E, Schmidt M, Stuerwald S (eds) Second international symposium on ultra high performance concrete, Kassel, pp 425–432
9. Fehling E, Schmidt M, Geisenhanslueke C (eds) (2004) Ultra high performance concrete (UHPC). In: Proc international symposium on UHPC, Kassel, Germany, 13–15 Sept 2004, 868 pp
10. Fehling E, Schmidt M, Stuerwald S (eds) (2008) Ultra high performance concrete (UHPC). In: Proc second international symposium on UHPC, Kassel, Germany, 3–5 March 2008, 902 pp
11. Graybeal BA, Davis M (2008) Cylinder or cube: strength testing of 80 to 200 MPa (11.6 to 29 ksi) ultra-high-performance fiber-reinforced concrete. ACI Mater J 105(6):603–609
12. Graybeal BA, Tanesi J (2007) Durability of an ultrahigh-performance concrete. J Mater Civ Eng 19(10):848–854
13. Habel K, Viviani M, Denarie E, Bruehwiler E (2006) Development of the mechanical properties of an ultra-high performance fiber reinforced concrete (UHPFRC). Cem Concr Res 36(7):1362–1370
14. Kim DJ, El-Tawil S, Naaman AE (2008) Rate-dependent tensile behavior of high performance fiber reinforced cementitious composites. Mater Struct 42(3):399–414
15. Kim DJ, Wille K, Naaman AE, El-Tawil S (2011) Strength dependent tensile behavior of strain hardening fiber reinforced concrete. In: Proceedings of HPFRCC 6, Ann Arbor, MI, 20–22 June 2011
16. Ma J, Dehn F, Koenig G (2003) Autogenous shrinkage of self-compacting ultra-high performance concrete (UHPC). In: International conference on advances in concrete and structures, Xuzhou
17. Maeder U, Lallemant-Gamboa I, Chaignon J, Lombard J-P (2004) Ceracem, a new high performance concrete: characterisations and applications. In: First international symposium on ultra high performance concrete, Kassel, pp 59–68
18. Matsubara N, Ohno T, Sakai G, Watanabe Y, Ishii S, Ashida M (2008) Application of a new type of ultra high strength fiber reinforced concrete to a prestressed concrete bridge. In: Second international symposium on ultra high performance concrete, Kassel, pp 787–794
19. Moeller A (2008) Use of UHPC in offshore wind turbine foundations. In: Second international symposium on ultra high performance concrete, Kassel, pp 863–869
20. Monai B, Schnabl H (2008) Practice of UHPC in Austria. In: Second international symposium on ultra high performance concrete, Kassel, pp 839–846
21. Mueller U, Meng B, Kuehne H-C, Nemecek J, Fontana P (2008) Micro texture and mechanical properties of heat treated and autoclaved ultra high performance concrete (UHPC). In: Fehling E, Schmidt M, Stuerwald S (eds) Second international symposium on ultra high performance concrete, Kassel, pp 213–220
22. Naaman AE (1992) SIFCON: tailored properties for structural performance. In: Reinhardt HW, Naaman AE (eds) High Performance fiber reinforced cement composites, Rilem proceedings 15. E & FN Spon, London, pp 18–38
23. Naaman AE, Najm H (1991) Bond-slip mechanisms of steel fibers in concrete. ACI Mater J 88(2):135–145

24. Naaman AE, Wille K (2010) Some correlation between high packing density, ultra-high performance, flow ability, and fiber reinforcement of a concrete matrix. In: BAC2010—2nd Iberian congress on self compacting concrete, University of Minho, Guimaraes, 1–2 July 2010

25. Richard P, Cheyrezy M (1995) Composition of reactive powder concretes. Cem Concr Res 25(7):1501–1511

26. Rossi P (2000) Ultra-high performance fibre reinforced concrete (UHPFRC): an overview. In: Proceedings of fifth RILEM symposium in fibre-reinforced concretes (FRC)-BEFIB' 2000, pp 87–100

27. Rossi P (2008) Ultra high performance concretes—a summary of the current knowledge. Concrete International, February, pp 31–34

28. Roy DM, Gouda GR, Bobrowsky A (1972) Very high strength cement pastes prepared by hot pressing and other high pressure techniques. Cem Concr Res 2:349–366

29. Scheydt J, Herold G, Mueller HS, Kuhnt M (2008) Development and application of UHPC convenience blends. In: Second international symposium on ultra high performance concrete, Kassel, pp 69–76

30. Teichmann T, Schmidt M (2004) Influence of the packing density of fine particles on structure, strength and durability of UHPC. In: First international symposium on ultra high performance concrete, Kassel, pp 313–323

31. Wille K, Naaman AE (2010) Bond stress slip hardening behavior of steel fibers embedded in ultra high performance concrete. In: 18th European conference on fracture, Dresden, 30 Aug–3 Sep 2010

32. Wille K, Kim DJ, Naaman AE (2011) Strain-hardening UHP-FRC with low fiber contents. Mater Struct 44(3):583–598

33. Wille K, Naaman AE, El-Tawil S (2011) Optimized ultra-high performance fiber reinforced concrete mixtures with twisted fibers exhibit record performance under tensile loading, in print, Concrete International, 2011

34. Wille K, Naaman AE, Parra-Montesinos GJ (2011) Ultra high performance concrete with compressive strength exceeding 150 MPa (22 ksi): a simpler way. ACI Mater J 108(1):46–54

35. Yudenfreund M, Skalny J, Mikhail RS, Brunauer S (1972) Hardened portland cement pastes of low porosity, II. Exploratory studies. Dimensional changes. Cem Concr Res 2(3):331–348